CHAPTER-3

SIGNATURE OF MONSOON VARIATION AND VEGETATIONAL CHANGE IN SIWALIK

3.1 Introduction

Carbon isotope ratio of soil carbonate is determined mainly by the type of vegetation sustained by the soil since the carbon derived from plant respiration and vegetation decay (soil respiration) is the dominant source of soil-CO_2, which leads to soil carbonate. Based on the carbon isotope ratio of soil carbonates from Pakistan and Nepal Siwaliks, it was shown that a major shift in vegetation (from a pure C_3 regime to C_4 dominant environment) occurred around 7 Ma ago (Quade et al., 1989; 1995). Later, the timing of shift in vegetation in Pakistan Siwalik was questioned by Morgan et al. (1994) who showed presence of C_4 grasses as early as 10 Ma based on carbon isotope ratio of tooth enamel. Carbon isotope ratio of alkanes extracted from soil organic matter also showed presence of C_4 plants at around 9 Ma (Freeman and Colarusso, 2001).

In Pakistan Siwalik, the above-mentioned C_3 to C_4 transition coincides with ^{18}O enrichment in soil carbonate, which was attributed to an increase in summer monsoon strength (Quade et al., 1989). However, $\delta^{18}O$ of soil carbonate is a function of several variables, such as temperature of carbonate formation, amount effect in rainfall, source of moisture, shifts in seasonality etc. (Quade et al., 1995; Quade and Cerling, 1995; Stern et al., 1997). In addition, the amount of rainfall over a soil regime and $\delta^{18}O$ of the corresponding soil carbonate is governed by the geographical configuration of the site during the formation of palaeosol. Thus, interpretation of $\delta^{18}O$ changes in soil carbonates is quite complex and it is not clear if the $\delta^{18}O$ increase in Pakistan Siwalik can be immediately explained by an increase in rainfall. In a later paper, Quade and Cerling (1995) also pointed that out increase in monsoon rainfall should cause depletion in oxygen isotope ratio and not enrichment as observed.

The presence of extensive Siwalik exposures in many parts of present-day India provides an opportunity for further studies on this topic. The present work was aimed to document the timing and nature of C_4 grass expansion in the Indian Siwaliks and its possible relationship to changes in rainfall. We present an investigation carried out on three Siwalik sections, two from the Kangra sub-basin (Ranital and Kotla) and one from the Subathu sub-basin (Haripur Khol) in Himachal Pradesh, India (Fig 2.1). These two areas are located in a region expected to be sensitive to changes in monsoon pattern because the seasonal rainfall in this part is very high (550 mm during SW monsoon;

Indian Meteorological Department, 1970) with closely spaced isohyets (Rao, 1976). Therefore, a small shift in monsoon pattern is expected to result in major change in rainfall here. Isotopic studies from such an area can help in deciphering past changes in monsoon circulation and in assessing their relation with the expansion of C_4 grasses.

3.2 Results

We identified six palaeosols in Ranital with easily discernible top and bottom parts where they are in contact with sandstone beds (see Fig.6.2); all these soils contain nodular soil carbonate. This allowed us to study the isotopic variation as a function of depth in a *single* soil profile.

The mean $\delta^{13}C$ values of soil carbonate nodules from six individual soil profiles from Ranital are −11.1 ± 0.3 ‰, −10.9 ± 0.5 ‰, −10.4 ± 1.0 ‰, −11.1 ± 0.6‰, −11.0 ± 0.4‰, − 11.1 ± 0.6, (n=2 to 4). The values are tightly clustered except one deviant sample with unusual enrichment (−5‰) (Table 3.1; Fig.3.1).

$\delta^{13}C$ of soil carbonate nodules in the Ranital section (corresponding to 11 Ma to 6 Ma) ranges from −11.5 ‰ to −7.8 ‰ (Table 3.2), whereas in the Kotla section (corresponding to 11 Ma to 6.5 Ma) it ranges from −12.2 ‰ to −9.3 ‰ (Table 3.2; Fig.3.2a). Correspondingly, $\delta^{13}C$ values of organic matter range from −24.7 ‰ to −26.3 ‰ in the Ranital section and −23.7 ‰ to −25.6 ‰ in the Kotla section (Table 3.2; Fig.3.2c). In these sections, the difference between $\delta^{13}C$ of organic matter and the soil carbonate, $\Delta(\delta^{13}C)$, lies within 14.9 ± 1 ‰. In the Haripur Khol section (corresponding to 6 Ma to 0.5 Ma) $\delta^{13}C$ of soil carbonate ranges from −4.8 ‰ to +2.4 ‰ (Table 3.2; Fig.3.2a). The corresponding $\delta^{13}C$ of the soil organic matter lies between −18.2 ‰ and −24.3 ‰ (Table 3.2; Fig.3.2c); the mean $\Delta(\delta^{13}C)$ in the Haripur Khol section is 19.7 ± 1.9 ‰.

The variability in $\delta^{13}C$ values of soil carbonate and organic matter is higher in Haripur Khol (post 6 Ma) compared to Kangra valley (Ranital and Kotla; pre-6 Ma). In Haripur Khol, the average $\delta^{13}C$ is −2.3 ± 1.7 ‰ (n=28), whereas for Kangra valley the mean value is −10.3 ± 1.3 ‰ (n=50). The average $\delta^{13}C$ of organic matter from Kangra valley, is −25 ± 0.7 ‰ (n=21) and for Haripur Khol it is −21.9 ± 1.9 ‰ (n=30) (Table 3.3).

As in the case of carbon isotopic ratio, oxygen isotope ratio of soil carbonate from a soil profile does not vary significantly with depth, except for marginal enrichment near the surface (Fig.3.1). The mean $\delta^{18}O$ values of nodules from six individual soil profiles from Ranital are -9.2 ± 0.6 ‰, -8.9 ± 0.5 ‰, -8.0 ± 1.3 ‰, -8.8 ± 0.8 ‰ -8.9 ± 0.2‰, -10.7 ± 0.8 ‰.

The isotopic data from the three sections (Haripur Khol, Ranital and Kotla) along with the age of the samples (see section 2.2 for discussion on age) can be combined to make a composite plot representing regional time variation of carbon and oxygen isotope ratios (Fig.3.2a, b, c). The composite plot for $\delta^{13}C$ shows a major change at about 6 Ma when the values become more positive by about 8 ‰. In the composite plot, the oxygen isotope ratio shows three evolutionary phases (indicated by three solid lines in Fig 3.2b). At around 10.5 Ma, $\delta^{18}O$ is characterized by highly depleted value of about -10 ‰; it tends towards more positive side with decrease in age, reaching -6.6 ‰ at around 6.5 Ma. Subsequently, the isotope ratio is characterized by a sharp depletion going up to -9 ‰ at 6.0 Ma and then a second phase of enrichment reaching -6.5 ‰ at around 2 Ma. These indicate two phases of depletion occurring around 10.5 Ma and 6.0 Ma punctuated by a period of maximum enrichment at around 6.5 Ma. Though the $\delta^{18}O$ values show definite trend with time, they are also characterized by scatter at the same stratigraphic depth, which complicates the interpretation.

3.3 Discussion

3.3.1 Information on vegetation change from carbon isotope ratio of soil carbonate and associated organic matter

Based on carbon isotope ratio, plants can be divided into two main photosynthetic pathways, C_3 and C_4, whose isotopic ratios are quite different. The majority of plants, comprising trees, shrubs, cool–season grasses, etc., follow C_3 pathway. The $\delta^{13}C$ of C_3 plants vary over a large range: -20 ‰ to -35 ‰ but the average is well constrained at -26.7 ‰. For C_4 type of plants (grasses), $\delta^{13}C$ values range from -6 ‰ to -19 ‰, with an average of about -13 ‰ (Cerling et al., 1997). Plant debris and associated bio-organic residues get incorporated in the soil (especially after death of the plants) and constitute the soil organic matter, which preserves the mean carbon isotopic composition of the contemporary vegetation with little or no fractionation. The soil carbonate forms from soil solution that uses soil CO_2 derived from oxidation of soil organic matter and plant respiration. In this step, the carbonate gets enriched in ^{13}C with respect to the source carbon (Cerling, 1984) due to two processes, namely, diffusion of CO_2 and equilibrium fractionation associated with carbonate precipitation from solution. The diffusion causes an enrichment of 4.4 ‰ in ^{13}C in soil CO_2 compared to the soil-respired CO_2. The equilibrium fractionation causes a further isotopic enrichment in soil carbonate depending on the temperature (for example, enrichment of 12.7‰ occurs at 0 °C and 9.8 ‰ at 25 °C). Assuming average soil temperature between 0 to 25 °C, the net increase in carbon isotopic ratio in transition from soil organic matter to soil carbonate [$\Delta(\delta^{13}C)$] should be in the range of about 14 ‰ to 17 ‰ if soil pCO_2 is high enough to prevent infiltration of atmospheric CO_2 (Cerling et al., 1989). However, occasionally $\Delta(\delta^{13}C)$ values lie beyond 14 ‰ to 17 ‰ limits even when the temperature is within 0 to 25 °C (Pendall and Amundson, 1990).

Table 3.1 *Carbon and oxygen isotope ratio of soil carbonate and carbon isotope ratio of associated organic matter from individual soil profile from Ranital Section of Kangra Valley. $\delta^{13}C$ and $\delta^{18}O$ are given relative to PDB in ‰ with errors of analysis: ±0.05 ‰ for carbonates and ±0.1‰ for organic carbon. Depth is measured from the top of each soil profile identified in the field by sharp transition to mudstone above.*

Sample No	Depth (cm)	$\delta^{13}C$ (‰)	$\delta^{18}O$ (‰)	$\delta^{13}C_{Org}$ (‰)	Sample No	Depth (cm)	$\delta^{13}C$ (‰)	$\delta^{18}O$ (‰)	$\delta^{13}C_{Org}$ (‰)
Profile-1					**Profile-4**				
PRL-010A1	30	−11.3	−8.7	−24.6	PRL-013A3	70	−10.6	−9.3	
PRL-010A2	55	−11	−8.7		PRL-013A1	30	−11.5	−8.2	
PRL-010A3	90	−11.5	−10	−25.3	**Profile-5**				
PRL-010A4	120	−10.7	−9.2	−25.2	PRL-019A	30	−11.0	−8.6	
Profile-2					PRL-019A1	45	−10.4	−9.0	−24.7
PRL-02B1	5	−4.9	−8.2		PRL-019A2	60	−11.4	−9.0	
PRL-02B2	30	−11.4	−9.2		PRL-019A3	90	−10.4	−8.8	−24.7
PRL-02B3	55	−10.9	−8.8		**Profile-6**				
PRL-02B4	95	−11.4	−9.4		PRL-017A	30	−11.3	−11.1	
Profile-3					PRL-017C	50	−10.5	−11.2	
PRL-03A01	30	−9.5	−6.6		PRL-017D	80	−11.1	−9.8	
PRL-03A0	35	−9.5	−7.1						
PRL-03A4	70	−11.2	−8.8						

Table 3.2 *Carbon and oxygen isotope ratio of soil carbonate and carbon isotope ratio of associated organic matter from Ranital, Kotla and Haripur Khol section. Age of each sample is determined by interpolation between palaeomagnetically dated horizons.*

Ranital Section

Sample No.	Age (Ma)	$\delta^{13}C$ Carb	$\delta^{18}O$ Carb.	$\delta^{13}C$ Org
PRL-02B2	10.9	−11.4	−9.2	nd
PRL-02B3	10.9	−10.9	−8.8	nd
PRL-02B4	10.9	−11.4	−9.4	nd
PRL-01	10.9	−11.4	−8.8	nd
PRL-1	10.9	−10.8	−8.7	−25.0
PRL-010A1	10.0	−11.3	−8.7	nd
PRL-010A2	10.0	−11.0	−8.7	nd
PRL-010A3	10.0	−11.5	−10.0	nd
PRL-010A4	10.0	−10.7	−9.2	nd
PRL-04A	9.7	−10.9	−7.8	nd
PRL-011	9.5	−11.2	−8.1	nd
PRL-2	9.5	−10.7	−7.9	−25.3
PRL-013A1	9.4	−11.5	−8.2	nd
PRL-013A3	9.4	−10.6	−9.3	nd
PRL-022	9.4	−11.5	−8.1	nd
PRL-017A	9.3	−11.3	−11.1	nd
PRL-017C	9.3	−10.5	−11.2	nd
PRL-017D	9.3	−11.1	−9.8	nd
PRL-06	9.1	−10.7	−8.7	−24.8
PRL-019A	9.0	−11.0	−8.6	nd
PRL-019A1	9.0	−10.4	−9.0	nd
PRL-019A2	9.0	−11.4	−9.0	nd
PRL-019A3	9.0	−10.4	−8.8	nd
PRL-3	8.8	−9.9	−7.2	−25.1
PRL-024	8.8	−10.8	−9.3	nd
PRL-026	8.7	−10.0	−7.8	nd
PRL-029	8.7	−10.7	−7.6	nd
PRL-032	8.1	−10.2	−8.7	−25.5
PRL-5	8.0	−10.1	−6.8	−25.2
PRL-037	7.4	−9.1	−8.0	nd
PRL-9	7.3	−8.3	−8.3	−24.7
PRL-042	7.1	−10.3	−7.7	nd
PRL-10	6.9	−9.5	−7.3	−25.9
PRL-11	6.2	−8.2	−6.6	−26.3
PRL-12	6.2	−8.5	−7.1	−25.9
PRL-047	6.1	−7.8	−7.5	−25.9
PRL-048	6.1	−10.6	−8.7	nd
PRL-050	6.0	−10.7	−7.5	nd

Kotla Section

Sample No.	Age (Ma)	$\delta^{13}C$ Carb.	$\delta^{18}O$ Carb	$\delta^{13}C$ Org.
KRL-2	10.5	−9.6	−9.7	nd
KRL-7	10.3	−9.3	−9.8	−23.7
KRL-11	9.2	nd	nd	−24.5
KRL-10	9.2	−10.8	−8.7	nd
KRL-13	8.8	−9.7	−9.4	−24.0
KRL-14	8.7	−10.8	−8.9	−25.0
KRL-17	8.5	−11.1	−9.4	−24.0
KRL-20	8.4	−12.2	−7.9	−24.0
KRL-21	7.9	−10.9	−7.9	−24.5
KRL-22	7.9	−10.7	−7.3	nd
KRL-24	7.1	−10.7	−7.4	−24.8
KRL-28	6.3	−9.4	−6.9	−24.2
KRL-29	6.2	−9.4	−6.8	−25.6

Haripur Khol section

Sample No.	Age (Ma)	$\delta^{13}C$ Carb	$\delta^{18}O$ Carb	$\delta^{13}C$ Org
HP-2(c)	5.9	−4.8	−8.7	−24.3
HP-3(c)	5.9	−4.2	−8.5	−23.9
HP-6(c)	6.0	−4.6	−8.8	−24.0
HP-8(c)	5.6	−2.6	−9.1	−23.3
HP-13(c)	5.4	−2.8	−9.5	−18.2
HP-15(c)	5.2	−2.8	−8.4	−21.1
HP-18(c)	5.0	nd	nd	−23.5
HP-A20(c)	4.8	−1.3	−8.2	−20.6

Haripur Khol Section

Sample No.	Age (Ma)	$\delta^{13}C$ Carb.	$\delta^{18}O$ Org.	$\delta^{13}C$ Org.	Sample No.	Age (Ma)	$\delta^{13}C$ Carb.	$\delta^{18}O$ Carb	$\delta^{13}C$ Org
HP-A23(c)	4.7	–4.5	–9.8	–23.8	HP-42(c)	2.7	nd	nd	–23.4
HP-21(c)	4.1	–3.2	–8.2	–22.3	HP-53(c)	2.6	0.4	–7.1	–22.3
HP-24(c)	3.9	–1.9	–7.6	–23.1	HP-54(c)	2.6	–2.6	–7.5	–21.3
HP-26(c)	3.8	–0.5	–6.6	–21.7	HP-55(c)	2.5	0.2	–7.6	–22.3
HP-30(c)	3.8	0.4	–7.0	–20.7	HP-57(c)	2.5	–2.6	–7.5	–22.6
HP-31(c)	3.7	–2.7	–8.2	–22.4	HP-61(c)	2.3	–2.2	–7.2	–22.4
HP-33(c)	3.6	–1.6	–8.6	–23.4	HP-64(c)	2.3	–2.3	–6.6	–23.0
HP-36(c)	3.3	–2.6	–7.2	–20.3	HP-65(c)	2.3	–3.5	–7.5	–23.0
HP-37(c)	3.3	–3.4	–7.2	–19.8	HP-66(c)	2.2	–3.3	–7.3	–18.2
HP-38(c)	3.2	–4.3	–8.3	–23.0	HP-70(c)	1.9	2.4	–6.8	–18.3
HP-39(c)	3.2	nd	nd	–18.2	HP-73(c)	1.9	1.4	–7.4	nd
HP-40(c)	3.0	0.9	–7.6	–23.5					

nd = not determined

In the Kangra valley, the carbon isotope ratio of individual palaeosols shows little variability with depth, except for one sample in soil Profile # 2 at depth ~5 cm (Table (3.1) (Fig.3.1)). The enriched value is probably due to contribution from atmospheric CO_2 ($\delta^{13}C = -7$ ‰) since the sample has a depth less than 25 cm (Cerling, 1984). The mean $\delta^{13}C$ (–10.9 ‰) obtained from the six profiles indicates that the source of carbon in the nodules is exclusively from plant-respired CO_2 (C_3 plant) if the samples are taken from a depth greater than ~25 cm (Fig.3.1) in a soil profile.

Data from the Kangra valley show that between ~10.5 to 6 Ma the floodplain was dominated by C_3 plants. Surprisingly, previous studies from neighboring Siwalik regions of Pakistan and Nepal showed that around 7 Ma, C_4 plants were already a major part of the ecosystem in the flood plain (Quade et al., 1989; 1995; Quade and Cerling, 1995). Unfortunately, paucity of pollen and fossil anatomy data from the Kangra valley prevents us from comparing isotopic data with vegetational record. For the interval between 6 Ma to 1.9 Ma the soil carbonate data from Haripur Khol show that the ecosystem was a mixture of C_3 and C_4 plants. The variability in $\delta^{13}C$ of soil carbonate and organic matter in Haripur Khol may be a reflection of the change in growing season conditions in a mixed C_3–C_4 environment, (see section 3.3.2 for further discussion).

The abundance of C_4 plants in Haripur Khol section can be estimated by isotopic mass balance from the data of either soil carbonate or organic matter by assuming that the mean $\delta^{13}C$ of C_4 plants is –13 ‰ and the mean $\delta^{13}C$ of C_3 plants is –25 ‰ (mean values of $\delta^{13}C_{org}$ measured from Ranital and Kotla sections). Such calculations show that the abundance of C_4 plants varied from 33 % to 78 % with an average of 53 ± 12 % (n=26) from soil carbonate data. In contrast, from soil organic matter of the same set of samples, estimate of C_4 abundance ranges from 5 % to 54 % with an average of 31 ± 12 % (n=26) (Fig.3.3). Ideally the two estimates should agree, but Fig.3.3 shows that for a given estimate of C_4 plant abundance from inorganic carbonate (take for example 50 %) the estimate from organic matter varies over a large range (from 10% to 55%). This indicates that in a mixed C_3–C_4 environment the $\delta^{13}C$ of residual organic matter cannot be taken as a proxy for the $\delta^{13}C$ of plant-respired CO_2. This is also clear from a plot of $\Delta(\delta^{13}C)$ (Fig.3.4a, derived from the composite plot: Fig.3.2.a, c) as a function of time which shows that the mean $\Delta(\delta^{13}C)$ for pre-6 Ma period is 14.9±1 ‰ whereas the value is 19.7±1.9‰ for post-6 Ma period. Possible causes of this variation are explored below.

3.3.2 Relationship between $\delta^{13}C$ values of soil carbonate and soil organic matter

The difference between abundance of C_4 plants calculated from data of soil carbonate and soil organic matter can be explained by the source-controlled model proposed by Wang and Follmer (1998), which modifies the assumption of Cerling regarding source of CO_2 (1984). According to the Wang-Follmer model, plant residue biomass contributes to soil organic matter whereas plant-respired CO_2 provides carbon source for soil carbonate, the respiration being vigorously active during the growing season. Thus the carbon isotope ratio of soil organic matter represents annual-average C_3/C_4 biomass content, whereas soil carbonate is more representative of growing-season plant respiration.

In a mixed C_3-C_4 environment if the growing season favors C_4 plant respiration, relatively more CO_2 would be produced from C_4 plants compared to that expected from the C_3-C_4 ratio in the residual organic matter. Therefore, the $\delta^{13}C$ value of soil CO_2 will be higher than the $\delta^{13}C$ value of the residual organic matter, and soil carbonate from such enriched soil CO_2 would make $\Delta(\delta^{13}C)$ larger than 14 ‰. Reverse case would occur if the growing season favours C_3 plant respiration.

In the Haripur Khol section, even though C_3 plants were dominant contributors of the soil organic matter, C_4 plant respiration was probably more active in the growing season compared to that of coexisting C_3 plants, which resulted in $\Delta(\delta^{13}C) > 14$ ‰ (Fig. 3.4a). It is of interest to note that the $\Delta(\delta^{13}C)$ in the Haripur Khol section show wide fluctuations (16.4 to 24.4 ‰) with age. There are two major swings towards higher value- at around 4 Ma and 2.6 Ma, thus indicating higher C_4 respiration. Lower values of $\Delta(\delta^{13}C)$ at around 3.2 Ma and 2.2 Ma may reflect the reverse condition. It is apparent that accurate estimates of these changes may have climatic implications. We note that each data point refers to a single soil profile, which represents time-averaged record over ~ 1,000 to 10,000 yr (Retallack, 2001a).

Table 3.3 *Carbon isotope ratio difference between soil carbonate and associated soil organic matter* [$\Delta(\delta^{13}C) = \delta^{13}C_{SC} - \delta^{13}C_{Org}$].

Ranital Section			**Kotla Section**			**Haripur Khol Section**		
Sample No	Age (Ma)	$\Delta(\delta^{13}C)$	Sample No	Age (Ma)	$\Delta(\delta^{13}C)$	Sample No.	Age (Ma)	$\Delta(\delta^{13}C)$
PRL-1	10.9	13.9	KRL-7	10.3	14.4	HP-2(c)	5.9	19.5
PRL-2	9.5	14.3	KRL-10	9.2	14.0	HP-3(C)	5.9	19.7
PRL-06	9.1	14.1	KRL-13	8.8	14.3	HP-6(c)	6.0	19.4
PRL-3	8.8	14.9	KRL-14	8.7	14.2	HP-8(c)	5.6	20.7
PRL-032	8.1	15.3	KRL-21	7.9	14.0	HP-15(c)	5.2	18.3
PRL-5	8.0	15.1	KRL-24	7.1	14.1	HP-A20(c)	4.8	19.3
PRL-042	7.1	15.6	KRL-28	6.3	16.2	HP-A23(c)	4.7	19.3
PRL-10	6.9	15.5	KRL-29	6.2	14.8	HP-21(c)	4.1	19.1
PRL-11	6.2	16.9				HP-24(c)	3.9	21.2
PRL-12	6.2	16.9				HP-26(c)	3.8	21.2
Haripur Khol section								
Sample No	Age (Ma)	$\Delta(\delta^{13}C)$)	Sample No	Age (Ma)	$\Delta(\delta^{13}C)$	Sample No	Age (Ma)	$\Delta(\delta^{13}C)$
HP-30(c)	3.8	22.4	HP-38(c)	3.2	18.7	HP-61(c)	2.3	20.2
HP-31(c)	3.7	19.7	HP-40(c)	3.0	24.4	HP-64(c)	2.3	20.7
HP-33(c)	3.6	21.8	HP-53(c)	2.6	22.7	HP-65(c)	2.3	19.5
HP-36(c)	3.3	17.7	HP-54(c)	2.6	18.7	HP-66(c)	2.2	14.9
HP-37(c)	3.3	16.4	HP-55(c)	2.5	22.5	HP-70(c)	1.9	20.7

Therefore, any inference regarding variations in growing season conditions would refer to average climatic fluctuations over this interval.

In this context it may be mentioned that climatic fluctuations have also been inferred from variation of oxidation, hydroxylation and humification index of

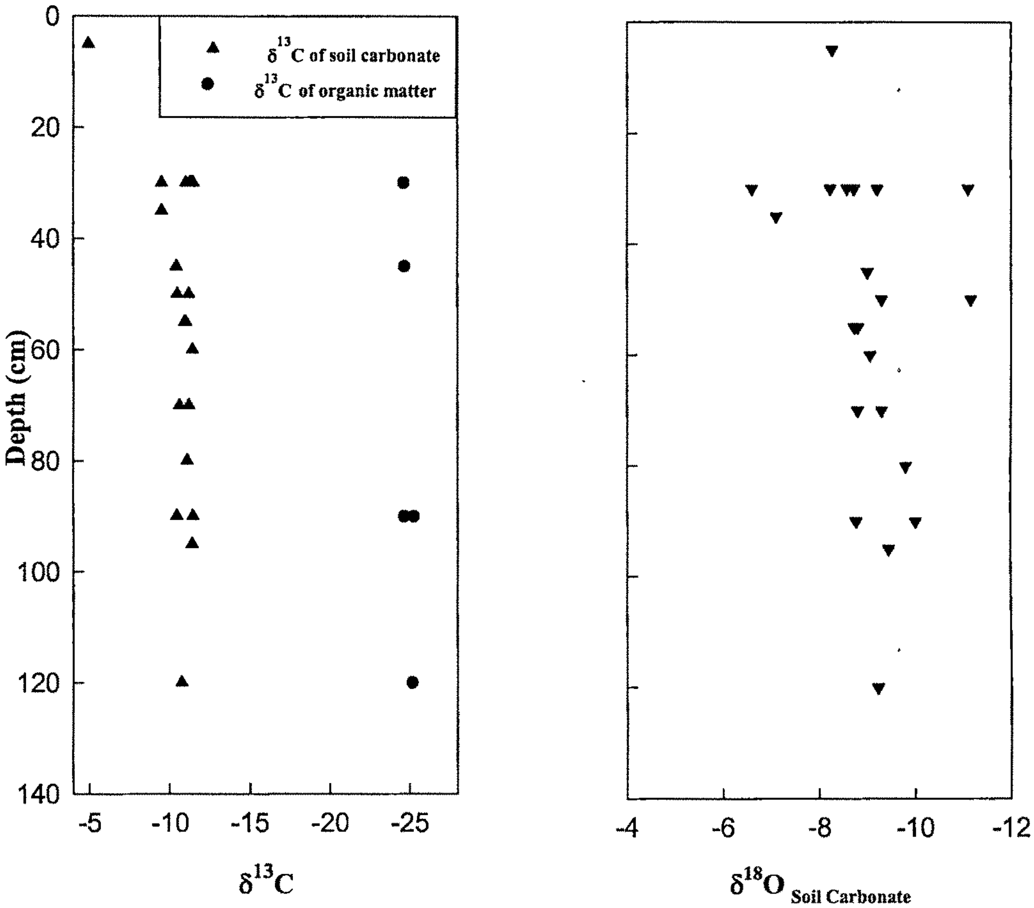

Fig.3.1 *Carbon and oxygen isotope ratio variation in soil carbonate taken from various depths within individual soil profiles (total 6) from Ranital section, Kangra valley. The carbon isotope ratio shows little variation with depth except one point ($\delta^{13}C$= –5‰), which may represent dominant atmospheric CO_2 contribution in soil CO_2. $\delta^{13}C$ values are consistent with C_3 type of plants in the soil. Oxygen isotope ratio shows enrichment as one moves towards the surface which may be due to evaporation of water from the top surface of the soil.*

Haripur Khol palaeosols. The indices are based on selective saturation levels of induced magnetic field, inorganic and organic carbon content, and Rb/Sr ratios. Variations in the indices indicate large-scale climate changes within the Pliocene-Pleistocene time span, with warm-humid climate during early Pliocene and intermediate phase during the early mid-Pliocene and warm oxidative phase during the mid to late Pliocene. The early-mid Pleistocene was characterized by a cold phase (Sangode et al., 2001).

Color and maturity of palaeosols also show evidence of climate change during the Pliocene-Pleistocene time period. Between 5.3 and 2.6 Ma, warm and humid climate

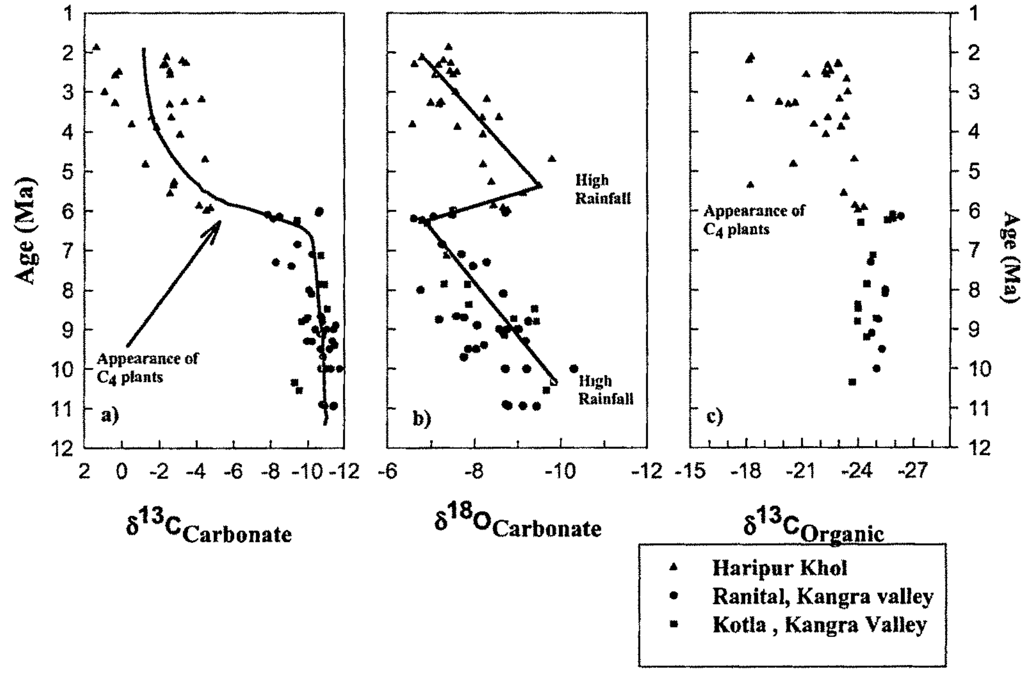

Fig.3.2 *Composite plot of isotope ratios against age of soil carbonate nodules from three sections (Ranital, Kotla and Haripur Khol) a) Carbon b) Oxygen and c) Organic matter from the same nodules. Carbon isotope ratio of soil carbonate and associated organic matter indicates that vegetation was entirely of C_3 type from 11 to 6 Ma. Post 6 Ma time is marked by appearance and expansion of C_4 grass. Oxygen isotope composition shows stepwise variation with probable peak at ~10.5 Ma and a clear peak at ~6 Ma. These variations are attributed to change in monsoon rainfall. The solid lines are drawn to guide the eye.*

is inferred from the formation of red Alfisols with soil carbonate and Fe nodule and strong illuviation of clay forming well-developed Bt horizons. After 2.6 Ma, formation of poorly developed yellow soils with commonly occurring nodular soil carbonate and calcite material disseminated in the ground mass indicate slightly cooler and drier climate (Thomas et al., 2002).

Fortunately a different record of monsoon variation in Plio-Pleistocene period is available from sea sediments, which gives us an opportunity to compare our results. The relative abundance variation of radiolarian species *Actinomma* in the Arabian Sea, a marine proxy for upwelling caused by monsoon winds, shows variation after 6 Ma with peaks around 4.7, 3.8, 3 and 2.2 Ma (Prell et al., 1992). Although there is no one to one correlation between the abundance peak of radiolarian species and higher value of $\Delta(\delta^{13}C)$, but overall, a monsoon change interpretation seems to agree with the observed

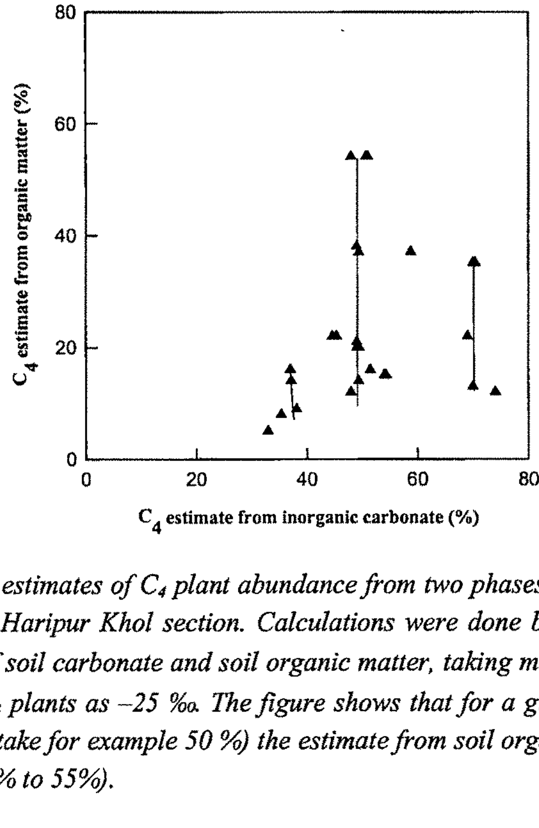

Fig.3.3 *Cross plot of estimates of C_4 plant abundance from two phases, soil carbonate and soil organic matter from Haripur Khol section. Calculations were done by isotopic mass balance and using the data of soil carbonate and soil organic matter, taking mean $\delta^{13}C$ of C_4 plant as –13 ‰ and that of C_3 plants as –25 ‰. The figure shows that for a given estimate of C_4 plant from soil carbonate (take for example 50 %) the estimate from soil organic matter varies over a large range (from 10% to 55%).*

$\Delta(\delta^{13}C)$ change for the post-6 Ma period (Fig.3.4a and Fig. 3.4b.). In case of Kangra valley, despite changes in climatic condition from 10.5 Ma to 6.5 Ma, as discussed later, the $\Delta(\delta^{13}C)$ value is nearly constant at 14 ‰ because only C_3 type of plants dominated the region at that time (Fig.3.4). This is consistent with Cerling's model (Cerling, 1984), which shows that for a single type of plants (in this case C_3) the change in soil respiration rate does not affect $\delta^{13}C$ significantly provided soil respiration rate is high.

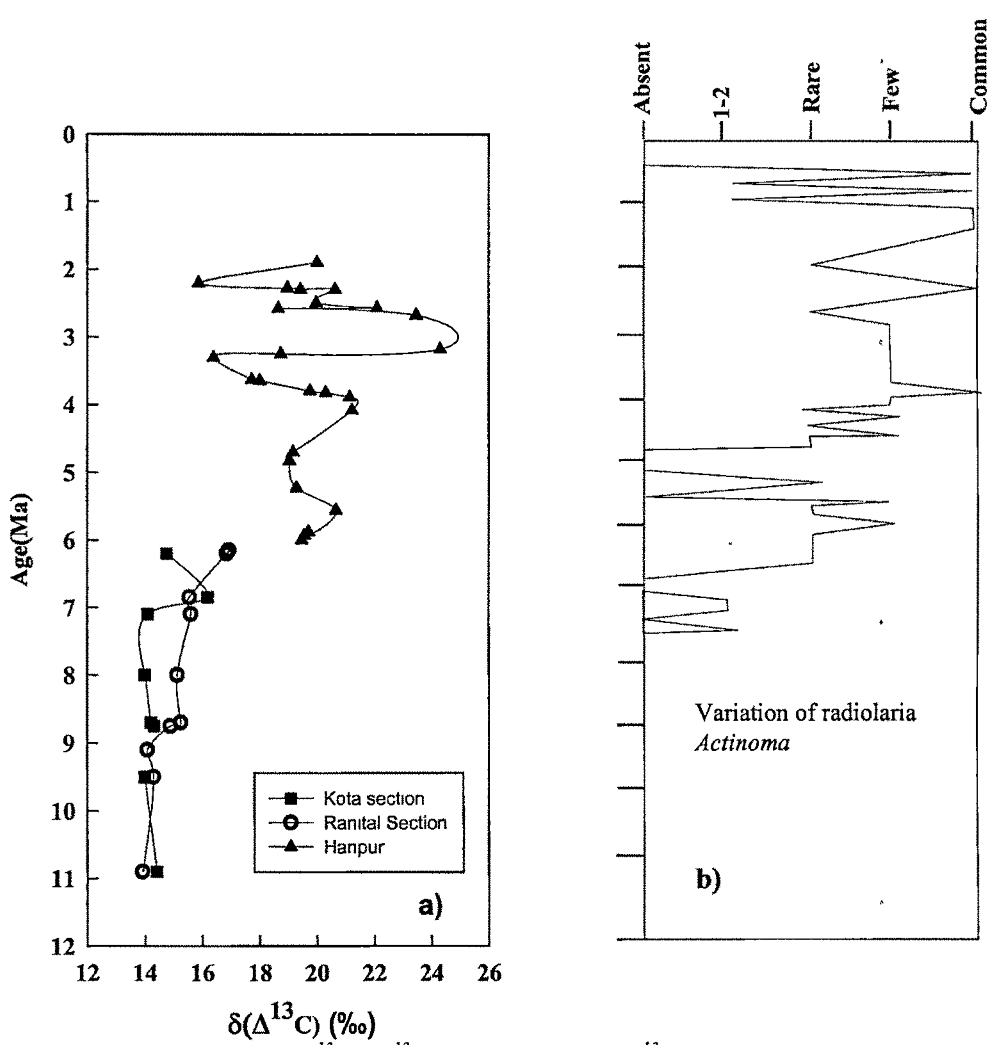

Fig. 3.4 a) *Variation of $\Delta(\delta^{13}C)$ ($\delta^{13}C$ soil carbonate – $\delta^{13}C$ organic matter) through time. In Ranital and Kotla $\Delta(\delta^{13}C)$ is 14.9±1‰ which is well within the prediction of diffusion-production model (Cerling, 1984). However, in Haripur Khol mean $\Delta(\delta^{13}C)$ is 19.7±1.9‰, which is beyond the predicted value of diffusion-production model. The variation of $\Delta(\delta^{13}C)$ in Haripur Khol is probably caused by growing season variation induced by climatic change. Variation is absent in pre 6 Ma period since only C_3 type of plants were present at that time.* **b)** *Abundance variation of endemic upwelling radiolarian species Actinomma in the Arabian Sea indicating variation in monsoonal strength. Comparison between the variation of $\Delta(\delta^{13}C)$ and abundance of radiolarian species shows reasonable agreement during the last 5 Ma, but not exact correlation.*

3.3.3 Supporting evidence of growing season change in Haripur Khol

The pollen record from Haripur Khol section supports the interpretation of variation of growing season condition with time. Considering the relative frequency of ecologically significant taxa, four major stages of vegetation has been recognized in Haripur Khol (Phadtare et al., 1994). The stages are: I) 4 to 3.5 Ma, II) 3.5 to 2.7 Ma, III) 2.7 to 2.5 Ma, and IV) 2.5 to 1 Ma. During stage I, the vegetation was dominated by dry grassland. The variety of monoporate, psilate and distinctly microreticulate pollen morphotypes indicates that at least four prominent genera of Poaceae were thriving in this area. The presence of Amaranth/Chenopodiaceae along with members of Polypodiaceae and other ferns further shows that at a few places, these plants were thriving during rainy to early summer times. During stage II, there was significant drop in percentage of grass pollens associated with sudden rise of the spores of *Lycopodium* and polypodiaceous ferns. During the later half of this stage, significant rise in Amaranth/Chenopodiaceae and large concentration of *Ceratopteris* pores indicates a marshy or muddy condition. During stage III, consistent increase in the spores of *Lycopodium* along with regular presence of algal cysts as well as dicot pollens collectively suggest the existence of well-developed ponding conditions. Presence of Nymphaeaceae indicates shallow-water or seasonal lacustrine habitat. A large population of *Pinus* pollen, restricted only to this stage, also indicates a temperate to sub-tropical climate. During stage IV, which is marked by the presence of volcanic ash bed, the leaf tissues are found to be abnormally thick. The abnormal cell wall thickness at this stage is intriguing but could be due to response of the leaves to a cool and dry climate (Phadtare et al., 1994). Also, effect of a possible CO_2 concentration change cannot be ruled out (Retallack, 2001b).

The above discussion indicates that the post-4 Ma vegetational regime in this part of the Indian Siwalik carries signature of major climatic changes, which could have prompted variations in the C_3:C_4 ratio, the type of C_3/C_4 plants and growing season condition which was finally recorded in the $\Delta(\delta^{13}C)$ variation observed here (Fig.3.4).

3.4 Oxygen isotope ratios of soil carbonate

3.4a Source of scatter in data

Oxygen isotope ratio of soil carbonate depends upon the isotopic ratio of soil water derived from local precipitation. Hence the $\delta^{18}O$ of soil carbonate can be used to decipher the average isotopic composition of precipitation (Quade et al., 1989). However, in the near-surface zone, the isotopic ratio of soil water can be significantly enriched in ^{18}O due to evaporation (Amundson et al., 1989; Quade et al., 1989). The $\delta^{18}O$ analysis of nodules at different depths from six individual soil profiles from Kangra valley (Fig.3.1) shows such enrichment towards the top. Therefore, the ^{18}O-depleted values deeper in the profile would better represent the soil water.

In individual soil profiles, higher variability in oxygen isotope ratio compared to that of carbon isotope ratio may reflect differential infiltration of seasonal precipitation. Precipitation may penetrate differentially into a soil, with deeper infiltration during one season, and more run-off during another. Because seasonal differences can cause changes in isotopic composition of meteoric water, a preferential infiltration may result in soil water delta value different from that of the average local meteoric water (Mora et al., 1993). Similar explanation can be offered for variation of $\delta^{18}O$ observed at a given depth in the composite profile. However, the variation in the composite $\delta^{13}C$ profile is not due to this reason. The scatter in the pre-6 Ma period is due to combination of data from two locations (Ranital and Kotla) each having slightly different C_3 population with different delta values (–25.4‰ for Ranital and –24.4 ‰ for Kotla). The post-6 Ma period is characterized by a mixed C_3-C_4 regime with two sources of scatter: variation in the relative proportion of C_3 and C_4 plants in different soils and the growing season variability. Despite the scatter, signals of distinct change (in both $\delta^{18}O$ and $\delta^{13}C$) are easily discernible in these records.

3.4b Implication of $\delta^{18}O$ variation

A major assumption in the interpretation of $\delta^{18}O$ of soil carbonate is that it forms in isotopic equilibrium with the soil water. This can be tested if the soil temperature is known. As a first-order approximation, the soil temperature can be taken as the mean annual air temperature (T) of the location. The fractionation factor between calcium carbonate and water is given by (Friedman and O'Neil, 1977): $1000\ln\alpha^{\text{calcite}}_{\text{water}} = 2.78 \times 10^6 / T^2 - 2.89$ where $\alpha^{\text{calcite}}_{\text{water}} = (1000 + \delta^{18}O_{\text{calcite}})/(1000 + \delta^{18}O_{\text{water}})$. The $\delta^{18}O$ of rainwater in Kangra and Haripur Khol has not been measured but can be estimated from data pertaining to the Delhi region (IAEA, 2003). The mean annual weighted average $\delta^{18}O$ in Delhi rain is about –6 ‰ (relative to SMOW). Correcting for the continental effect (a decrease of about 0.4‰; Krishnamurthy and Bhattacharya, 1991) and enrichment effect (about 1 ‰) due to evaporation during recharge (Salomons et al., 1978) the $\delta^{18}O$ of soil water in Kangra can be estimated to be –5.4 ‰. Taking the mean annual temperature of Kangra and Haripur Khol to be about 23 °C (based on the meteorological data of Pathankot, which is 60 km from Kangra valley) Kangra soil carbonate is expected to have a $\delta^{18}O$ value of –7 ‰ (PDB), which is close to the observed mean value of the younger soil carbonates from both Kangra and Haripur Khol. The close agreement lends validity to the equilibrium assumption for the soil carbonate as well as the temperature estimate. The situation is complex when one wants to interpret the isotope data for the old soils since the past soil temperature has to be known or estimated.

Taking modern $\delta^{18}O$ value of the Kangra soil water (–5.4 ‰) as representative, a $\delta^{18}O$ value of ~ –10 ‰ (PDB) for soil carbonate (at 10.5 Ma) would require mean annual temperature of about 39 °C (using Friedman and O'Neil equation). This value is unrealistically high for the region and, therefore, temperature cannot be the cause for ^{18}O depletion at 10.5 Ma; the same argument holds for depletion observed at 6.0 Ma. Additionally, the geographical location of the site was not significantly different from that of today (Harrison et al., 1998) and, therefore, the mean temperature was probably similar to that of today.

We propose that the above-mentioned two phases of depletion in ^{18}O, which occurred around 10.5 Ma and 6.0 Ma, (Fig 3.2b) reflect an increase in the intensity of summer monsoon rainfall. The summer monsoon in North India is characterized by heavy rains during June, July, August and September and is caused by convective vortex of west-northwest moving depressions originating from the Bay of Bengal operating on moist oceanic air moving in the same direction. In contrast, during winter, dry continental air blows from the northeast, resulting in little rains except occasional precipitation in Kangra region due to western disturbances bringing moisture from the Mediterranean region. The winter rains are usually more enriched compared to summer rains as observed from the seasonal variation data of Delhi rains (IAEA, 2003). Furthermore, $\delta^{18}O$ of rainwater decreases with an increase in the amount of precipitation (IAEA, 2003). At low latitudes, the average monthly rainfall and the mean monthly $\delta^{18}O$ are usually negatively correlated, showing that an increase of 100 mm of precipitation is associated with a decrease in $\delta^{18}O$ by 1.5 ‰ (Yurtsever and Gat, 1981). Therefore, it can be argued that the two phases of depletion in oxygen isotopic composition of soil carbonate (i.e. during 10.5 Ma and 6.0 Ma) were the result of contemporary intensification of the summer monsoon, because intensified monsoonal wind system would generate more intense and frequent depressions (storms) and result in more rains. It is to be noted that Quade et al. (1989) also obtained depleted $\delta^{18}O$ values at about 10.5 Ma and in their composite profile, the maximum depletion occurs at about 9 Ma. Subsequently, the value increases and the scatter becomes too large to detect any signal. We obtained an increasing trend up to 6.5 Ma with an attendant swing after 5.5 Ma. This sharp change is probably present but not clearly recorded in the profile of Quade et al. (1989). One reason could be that, the Pakistan Siwalik is located at the farthest end of the Indian monsoon system and consequently may not be able to record minor oscillations, which may show up in Indian Siwalik.

3.5 Comparison of monsoon evolution with other proxies

It is natural to enquire if there are other proxies showing monsoon intensification signals in this time scale. In the marine regime, there are foraminiferas (e.g. *G. bulloides*), which are sensitive indicators of upwelling, whose strength is influenced by monsoon winds. Interestingly, a quantitative frequency analysis of *G. bulloides* from the Arabian sea shows high abundance values around 8 Ma, followed by gradual diminution around 5.5 Ma. This is succeeded by an increase at around 4.5 Ma that continued until today, with minor oscillations (Kroon et al., 1991) (Fig.3.5). Radiolarian assemblages also show onset of monsoon at 11.9 Ma (followed by weakening at 9.6 Ma) and an upwelling peak at around 4.7 Ma (Nigrini, 1991). The ~4.5 to 4.7 Ma monsoon intensification peak in ocean data is close to our proposed monsoon increase at ~6 Ma. Though *bulloides* data are somewhat different, the radiolarian increase during 11.9 to 9.6 Ma is close to the 10.5 Ma Siwalik peak. The time difference of about 1 Myr or less between the two systems could be due to dating errors inherent in the age control of the two systems.

Sedimentological evidences from Siwalik support our observation regarding changes in the Indian summer monsoon. The fluviatile sedimentation of the Himalayan Foreland Basin (HFB) was controlled by tectonics and weathering with a strong influence of climate. Kumar et al. (2003a) observed two major changes of sedimentation

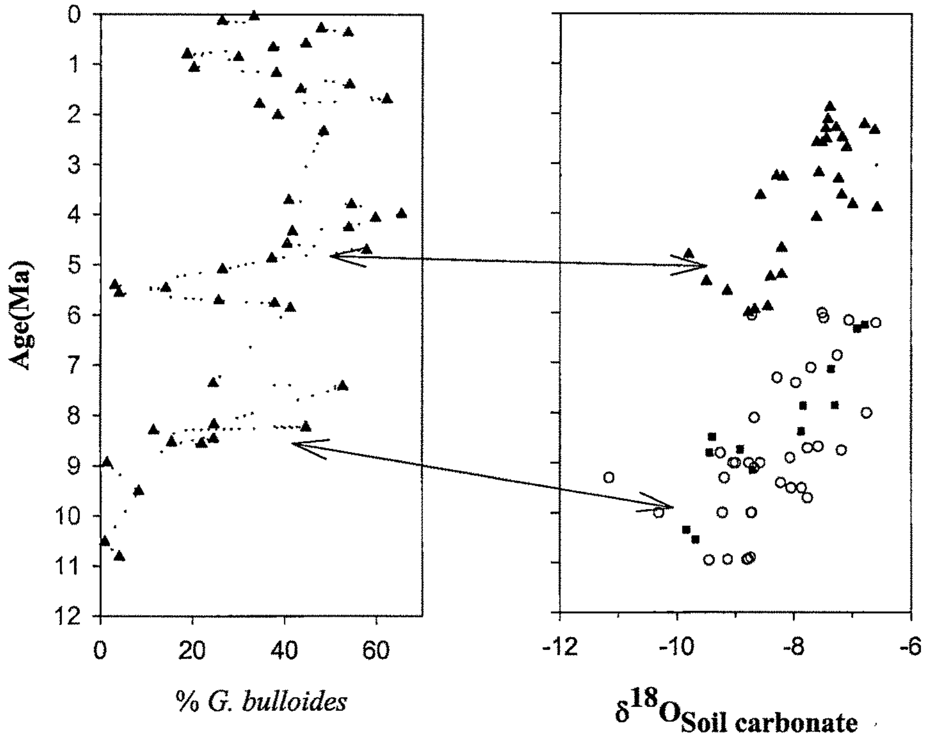

Fig.3.5 *Comparison between abundance variation of G. bulloides in Arabian Sea and oxygen isotope ratio variation of soil carbonates from Siwalik through time. Arrows show correlation of monsoon intensity between the two records.*

pattern and drainage organization at 10 Ma and 5 Ma and several minor interspersed events, reflecting environment of sedimentation during the entire 10 to 0.5 Ma period. The succession around 10 Ma is characterized by multistory sandstone with abundant erosional surfaces but no lateral accretionary surfaces, and low palaeoflow variability. These features indicate deposition in frequently avulsing large braided river system. Net sediment accumulation rate also increased by a factor of 2 to 3 at 10 Ma. This change may be due to uplift of source area coupled with intensified rainfall regime. Although increase in tectonism can produce high relief, more detritus transportation of sediment across the foreland basin requires enhanced discharge by large river systems, which can be brought about only by intense rainfall (Kumar, et al., 2003a). The evidence for increase in tectonism is provided by mineralogical studies, which show that the Central Crystalline zone suffered a major uplift in response to reactivation of the Main Central

Thrust (MCT) at around 10 Ma (Zaleha, 1997; Hisatomi, 1990; Ghosh and Kumar, 2000; White et al., 2001). In addition to the tectonic controls on basin fill, climate also exerted an influence on the overall distribution of grain size and rate of sediment supply to the basin. Formation of purple and brown colored palaeosols with calcareous nodules around 10 Ma suggests a humid warm climate. Fluvial architecture during this time also suggests a gradual increase in river size and its discharge. For example, mass accumulation rate in the Ganga basin shows rapid increase around 10 Ma (Metivier et al., 1999). From a host of such sedimentary features, it appears that precipitation in the Himalayan region increased at around 10 Ma.

Presence of gypsum needles in the Ranital section at around 6.5 Ma, noted during the present field excursion, indicates extreme aridity marking a weakened phase of the monsoon. This was quickly followed by widespread distribution and stacking of conglomerate and progradation of alluvial fans between 6 and 5 Ma, suggesting a broad catchment area with high basin relief (Kumar et al., 2003b) heralding the second phase of monsoon intensification. It provided a high volume of sediment resulting in distribution of coarse-grained sediments in the proximal part, and fine sediments in the distal part of the alluvial fan system.

In Siwalik sections of Pakistan and India, strata older than 8 Ma are characterized by thick amalgamated sandstone with minor occurrence of overbank deposits. The overbank deposits are characterized by deeply leached palaeosols lacking humic horizons. In contrast, the lithofacies younger than 8 Ma are characterized by abundant overbank deposits with shallowly leached palaeosols having significant humic horizons. This lithofacies contrast suggests that flooding and effective rainfall were considerably greater before 8 Ma (Burbank et al., 1993).

It is known that uplift of the Tibetan plateau had profound influence in the initiation of Asian monsoon system. However, there exists a great deal of uncertainty regarding the time of attainment of present day elevation of Tibetan plateau. Harrison et al. (1992) suggested that much of the elevation was attained ~8 Ma ago. In contrast, Coleman and Hodges (1995) argued that the Tibetan plateau was uplifted to its present elevation ~14 Ma ago. Supporting evidences for the latter are provided by studies of Edward et al. (1996) and Yin et al. (1994) suggesting uplift of High and Tethyan

Himalaya during the middle Miocene (17–11 Ma). Recent paleo-botanical evidence from the Namling basin (West of Lhasa) also indicates that the plateau had already attained its present elevation at around 15 Ma (Spicer et al., 2003). The bulk of the evidences thus favour an earlier timing for uplift of the Tibetan plateau.

Although the above studies provide a time constraint for plateau upliftment and consequent initiation of Monsoon, they do not necessarily imply *intensification* of the southwest monsoon. Burbank et al. (1996) showed that almost all the Siwalik sections from Pakistan to Nepal recorded acceleration in sedimentation and increase in subsidence at around 11 Ma. This increase in sediment flux to the Himalayan foreland basin was probably due to the combined action of intensified monsoonal precipitation and tectonic activity. In this context, our study provides support for enhanced precipitation at around 10.5 Ma.

3.6 Causes of C_4 plant appearance

It is well known that physiology of C_4 plants provides them with competitive advantage over C_3 plants when the ratio of atmospheric CO_2/O_2 concentration is low. Moreover, the ability to increase internal CO_2 concentrations allows C_4 plants to decrease their stomatal conductance, which effectively increases their water-use efficiency. Such adaptations provide advantages under hot, high-irradiance, water stressed conditions, where plants must close their stomata to prevent water loss, and in doing so they also reduce the ability to take CO_2 from the atmosphere. However, as they can concentrate CO_2 within the leaf they can continue photosynthesis without any hindrance. The above physiological considerations led Cerling et al. (1997) to propose that a lower concentration of atmospheric CO_2 operating in typical low latitude temperatures was the main cause of expansion of C_4 plants.

This proposition is compatible with observed lowering of the atmospheric CO_2 concentration in the Neogene period. Boron isotope ratios of foraminifera act as a proxy for surface ocean pH and indicate that atmospheric partial pressure of CO_2 was 4.5 times the present value at 21 Myr ago (Fig.1.2) (Spivack et al., 1993). Stomatal index variation of fossil leaves also shows a Late Miocene CO_2 decline in atmosphere (Fig.1.2) (Van Der Burg et al., 1993; Retallack, 2002). However, there are some recent studies, which are at variance with this proposition (Fig.1.2). As mentioned in the introduction, reconstruction of paleo-CO_2 concentrations from alkenones led Pagani et al. (1999) to rule out CO_2 change as the cause for C_4 expansion. Instead, they attributed this event to increasing seasonality and aridity (Pagani et al., 1999). Their model is based on the fact that C_4 expansion was always associated with changes in seasonal pattern of precipitation during late Miocene time. For example, evolutionary trends in mammals and floras from middle to late Miocene suggest a pattern of increasing seasonality and aridity in North America, Europe, Africa, Pakistan and Australia. Increase in $\delta^{18}O$ values of soil carbonates from Pakistan, Nepal, East Africa, Argentina and the eastern Mediterranean, as well as in $\delta^{18}O$ values of tooth enamel from Argentina and North America, suggest increasing evaporation and aridity preceding and accompanying the expansion of C_4 flora (Pagani et al., 1999).

Our study from the Indian Siwalik shows that hydrological change is not always accompanied by vegetational change. Around 10.5 Ma, monsoon was intensified and contemporary vegetation was characterized by C_3 type of plants. After 10.5 Ma, monsoon strength started diminishing and by 6.5 Ma it reached the weakest phase. But during this entire period (10.5 Ma to 6.5 Ma) the vegetation was exclusively of C_3 type. The intensification of monsoon after 6 Ma was accompanied by appearance of C_4 plants (Fig.3.3a, 3.3b). An intense monsoon implies not only high rainfall but also strong seasonality, and we think that this latter property could have helped in the invasion of C_4 plants.

It is, therefore, clear that monsoon was intensified first at 10.5 Ma and then at 6 Ma, but C_4 plants appeared only at around 6 Ma. This indicates that although a change in seasonality associated with strong monsoon was probably a controlling factor for the appearance of C_4 plants, this factor must have operated in tandem with CO_2 decline discussed above. It is likely that initial lowering of CO_2 created an environment for C_4 grasses that was facilitated by change in precipitational pattern and the expansion of C_4 plants in Indian Siwalik followed this combined change.

3.7 Conclusions

The evolution of southwest monsoon, which is the main source of precipitation in the Indian subcontinent, was not gradual. The monsoon system intensified with one probable peak at around 10.5 Ma and a clear onset at 6 Ma with peak at 5.5 Ma; after 5.5

Ma monsoon strength decreased and attained the modern–day condition with minor fluctuations. From 10.5 Ma to 6 Ma, the floodplain was exclusively dominated by C_3 plants. C_4 plants appeared after 6 Ma and this coincides with monsoon intensification. From 6 Ma to 1.8 Ma the vegetation was characterized by a mixture of C_3 and C_4 types of plants. The sudden appearance of C_4 plants at ~ 6 Ma probably reflects the compound effect of intensified monsoon and lowering of pCO_2 in the atmosphere.

Our studies demonstrate that in a mixed C_3-C_4 environment, estimates of abundance of C_3 and C_4 plants from soil carbonate and associated soil organic matter may differ. Because soil carbonate is derived exclusively from plant-respiration, this difference may be due to differential response of respiration by these two types of plants (C_3 and C_4) to growing season. The abundance estimate based on $\delta^{13}C$ of soil carbonate would, therefore, change if the growing season differs from time to time in response to climate fluctuations. Consequently, the difference in $\delta^{13}C$ values of soil carbonate and organic matter may provide a unique way to decipher past climatic change.